Adsorption and Decomposition Pathways of Cyanogen Halides on Si(100)−(2×1)

Evgueni B. Kadossov, P. Rajasekar, and Nicholas F. Materer*

Department of Chemistry, Oklahoma State University, Stillwater, Oklahoma 74078-3071

Received: May 30, 2003

The adsorption and surface reactions of ICN, BrCN, and ClCN on the Si(100)−(2×1) surface are studied using ab initio quantum calculations on single- and triple-dimer silicon clusters. These cyanogen halides can physisorb into an end-on molecular species that is bound through the N to the Si cluster via a dative bond. The adsorption energy of this dative bonded species is found to depend on the cluster size. This species can further react to form a side-on intermediate by reacting across the Si-dimer bond or can lose the halide group and form an adsorbed CN species. The adsorbed CN group can have N-bonded and C-bonded orientations, with the C-bonded configuration having the lowest energy. The side-on intermediate can react to an additional intermediate species in which the halide−carbon bond is broken and the C end of the CN group inserts into the Si-dimer bond. An adsorbed CN group can subsequently form from this insertion species. Once the reaction proceeds from the dative bonded species, no significant barriers are present and the lowest energy structure is predicted to form in agreement with experimental studies.

Introduction

The surface functionalization of group IV semiconductors, in particular Si(100), with organic molecules promises the opportunity to create devices that exploit combined properties of organic materials with conventional semiconductors. The adsorption of organic molecules to fine-tune the chemical and physical properties of the surface has applications in chemical sensors, biological recognition, and molecular and optical electronics.[1,2] To realize these applications, a fundamental understanding of the reactivity of the Si(100) surface toward various organic compounds is required. The adsorption and decomposition of many organic compounds containing N and O with the Si(100) surface have recently been reviewed.[3] One important feature of the Si(100) surface is the presence of Si dimers that act as electron acceptors and play a critical role in the adsorption chemistry of nitrogen-containing organic compounds.[4−6] To advance the current understanding of the CN function group, this article explores the adsorption and subsequent surface reactions of ICN, BrCN, and ClCN with the Si(100)−(2×1) surface using ab initio quantum calculations on single- and triple-dimer silicon clusters.

Hydrogen cyanide (HCN) and cyanogen (C_2N_2) have been studied in detail by M. C. Lin and co-workers on Si(100) and Si(111) surfaces.[7−9] Unlike the case of the XCN on Si(100) surface,[10,11] the addition of the adsorbed H atom complicates the surface chemistry by reacting with the CN functional group. For HCN, Lin and co-workers find that, at high exposures, HCN dimerizes and possibly polymerizes on the Si(100) surface at low temperatures.[9] Upon warming, iminium (HC−NH) and CN species are identified as decomposition products. In addition to HCN and organic nitriles, the adsorption of phenyl isothiocyanate,[12] acetonitrile,[13,14] and benzonitrile[15] have been studied experimentally on the Si(100) surface. At room temperature, the CN group undergoes a 1,2-dipolar addition reaction across the Si-dimer bonds, forming a surface product that contains a four-membered Si_2NC ring. For acetonitrile, near-edge X-ray absorption fine structure spectroscopy indicates that other bonding geometries are present.[13]

The adsorption and thermal chemistry of the cyanogen halides (XCN, where X = I, Br, Cl) have been investigated using ultraviolet photoelectron spectroscopy (UPS) and X-ray photoelectron spectroscopy (XPS).[10,11] Briefly, UPS measurements show that the CN triple bond of the XCN species remains intact upon adsorption. XPS analysis of the C 1s photoelectron peak following low XCN exposures (0.2−0.3 L) at low temperatures (100 K) indicates that some molecular adsorption occurs. Upon annealing to room temperature, the XC bond of the molecularly adsorbed XCN species dissociates, leaving only the CN bond intact. BrCN and ClCN are observed to have a higher X−CN dissociation temperature than that found for ICN. Simultaneous changes in the C 1s and N 1s photoelectron peaks between 470 and 800 K support a model in which CN bond cleavage is correlated with silicon carbide and nitride formation.

Using ab initio quantum calculations on single-dimer silicon clusters, the adsorption and surface decomposition of ICN on the Si(100)−(2×1) surface has been modeled theoretically.[16] On these clusters, ICN can physically adsorb into an end-on molecular species that is bound through the N to the Si cluster via a dative bond. This species is found to react further to form either a dissociated state directly or a stable side-on intermediate by reacting across the dimer bond. Two dissociation states containing atomic I and the CN group are found. The CN functional group can bind to the silicon surface through either C or N end, with the former being the lowest energy product. HCN and its isomer HNC have been studied computationally on both single- and double-dimer silicon clusters.[7,17] Although some important differences are found between HCN and ICN adsorption chemistry,[16] the lowest adsorption energy structure contains a C-bonded CN functional group species bounded to one Si dimer atom with the halide or the H atom bound to the other dimer atom.

The work extends the previous investigations of the adsorption and decomposition processes of ICN on Si(100) surface[16]

* Corresponding author. Phone: (405) 744-8671. Fax: (405) 744-6007. E-mail: materer@okstate.edu.

10.1021/jp0306848 CCC: $27.50
Published on Web 12/10/2003

to BrCN and ClCN using the Gaussian 98 package.[18] Si(100)−(2×1) surface is modeled by both single-dimer (Si_9H_{12}) and triple-dimer ($Si_{21}H_{20}$) clusters. The Si_9H_{12} cluster is utilized to investigate adsorption geometries and transition states, while the larger, more computationally demanding $Si_{21}H_{20}$ clusters are used to assess cluster size dependent effects.

Computational Procedure

Energy calculations, geometry optimizations, and frequency calculations are performed using the hybrid density functional method that includes Becke's three-parameter nonlocal-exchange functional[19] with the correlation functional of Lee−Yang−Parr, B3LYP.[20] The 6-31G(d) all-electron split-valence basis set,[21] which includes the polarization *d*-function on non-hydrogen atoms, is employed for all BrCN and ClCN calculations. For the ICN calculations, the LanL2DZ basis, which includes the D95 double-ζ basis set,[22] combined with Hay and Wadt's effective core potential[23] is utilized for I. The larger 6-311++G-(2d,p) basis set is utilized in selected calculations to verify the suitability of the 6-31G(d) basis set. The adsorption energy is defined as the difference between the total electronic energy of the adsorption model and the isolated molecule and cluster. For both single- and triple-dimer clusters, all energies are reported without zero-point corrections. Frequency calculations confirm that the stable geometries have real vibrational frequencies. For the transition states, the optimized Gaussian 98 geometries contain only one imaginary normal mode. For all structures, atomic positions are optimized without geometry constraints. The buckling angle is calculated with respect to a plane that passes through the four Si atoms directly below the Si−Si dimer that is bonded to the cyanogen halide species.

The Si(100) surface is represented either as a single-dimer Si_9H_{12} or as a triple-dimer $Si_{21}H_{20}$ cluster. The Si_9H_{12} cluster has been utilized in the previous study of ICN[16] and HCN[7] adsorption on Si(100) surfaces. In addition, this cluster is used in studies of other nitrogen-containing compounds, such as ammonia and various amines.[24−28] However, the initial dative bonding geometry for ammonia and HCN is sensitive to the cluster size.[17,26] Size-dependent effects on both the resulting stable structures and selective transition states are investigated using the larger $Si_{21}H_{20}$ cluster.

Results and Discussion

Gas-Phase Isomerization. To ascertain the suitability of B3LYP/6-31G(d) for the molecular species, the isomerization of ClCN and BrCN is examined. The results for ICN are described in ref 16. The B3LYP/6-31G(d) isomerization energy for BrCN is within 10 kJ/mol of that in a MP2/6-31G(d) study[29] and within 6 kcal/mol of a calculation using a closed-shell single and double coupled-cluster method that includes a perturbational estimate of the effects of connected triple excitations (CCSD-(T)) with a 6-31G(p,d) basis set. Although the BrC bond length obtained using the B3LYP and the MP2 methods agree well, the B3LYP/6-31G(d) CN bond length is 0.03 Å shorter than that found using MP2/6-31G(d).[29] Differences in bond lengths between B3LYP/ 6-31G results and CCSD(T)/6-31G(d,p) results are within 0.01 Å. In addition, B3LYP/6-31G BrC and CN bond lengths for BrCN are within 0.01 Å of the experimental value determined by microwave spectroscopy.[30]

For ClCN, the isomerization energy obtained at the B3LYP/6-31G(d) level is within 2.5 kJ/mol of that calculated using CCSD(T) level with a cc-pVTZ basis set.[31] The bond lengths differences are less than 0.01 Å for both ClCN and ClNC. The final computed structure for ClCN also agrees favorably with the experimentally determined structure.[30,32] Thus, B3LYP/6-31G(d) method gives good agreement with both experimental and theoretical results for molecular BrCN and ClCN.

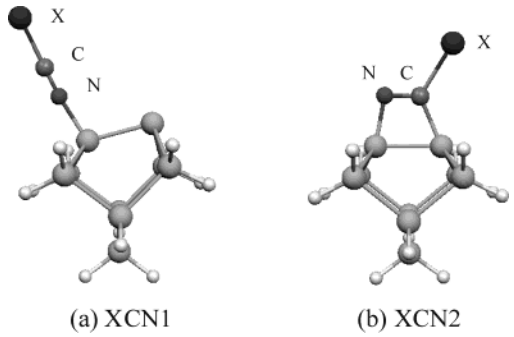

Figure 1. XCN derived adsorption models on the Si single-dimer cluster. (a) XCN1: XCN adsorbed on Si(100) surface in an end-on position. (b) XCN2: XCN adsorbed on Si(100) surface in a side-on position.

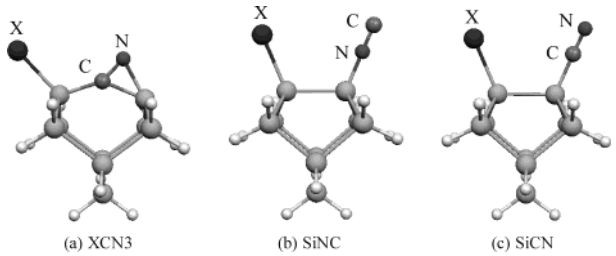

Figure 2. Additional XCN derived adsorption models on the Si single-dimer cluster. (a) XCN3: dissociated species X and CN adsorbed in a side-on position. Both the X−C and the silicon dimer bonds are broken. (b) SiNC: dissociated species X and NC adsorbed on Si(100) surface. (c) SiCN: dissociated species X and CN adsorbed on Si(100) surface.

XCN Adsorption on the Si(100) Surface. Possible adsorption structures for XCN on single-dimer clusters are shown in Figure 1. Without dissociation, the cyanogen halides can be adsorbed into two states: XCN1 and XCN2. In XCN1, the nitrogen lone pair forms a dative bond between the nitrogen end of the XCN molecule and the electrophilic (buckled-down) Si dimer atom. Even with constrained geometry optimizations, no stable binding geometry is found for an analogous geometry in which the lone pair of the halide binds to the electrophilic Si dimer atom. XCN2 is generated by the reaction of the CN group across the silicon dimer to achieve a side-on configuration. Following XC bond cleavage, Figure 2 illustrates three additional structures, XCN3, SiNC, and SiCN. The SiNC and SiCN configurations contain an intact CN functional group bonded to the Si dimer atom through either the N or C end. The halide is bonded to the Si dimer atom opposite the dimer atom bonded to the CN group. The XCN3 model has the C atom of the CN group inserted between the Si dimer atoms. The reported SiC distance for this species is measured with respect to the Si dimer atom bonded to the halide.

Geometry optimization at the B3LYP/6-31G(d) level for the XCN1, XCN2, SiNC, and SiCN adsorption models for ICN has been performed on single-dimer clusters for ICN.[16] To further verify the acceptability of the 6-31G(d) basis sets for this system, additional calculations are performed for ICN using the larger 6-311++G(2d,p) basis for the Si dimer atoms and the N and C species. XCN3, which has not been previously considered for ICN, is also included for completeness. The results are summarized in Table 1. The final geometry and total energy of these 6-31G(d) results are within 7 kJ/ mol of that found using the larger basis set. The largest relative error between these two sets is found for the dative bonded XCN1 structure. Consistent

TABLE 1: B3LYP-Calculated Geometries and Adsorption Energies (kJ/mol) for ICN Adsorption Structures on Single-Dimer Clusters[a]

		ICN1	ICN2	ICN3	SiNC	SiCN
R_{IC}	St	2.004	2.240			
	Ex	1.973	2.200			
R_{CN}	St	1.162	1.264	1.258	1.186	1.165
	Ex	1.159	1.266	1.261	1.179	1.161
R_{SiC}	St		1.953	1.866		1.852
	Ex		1.944	1.853		1.846
R_{SiN}	St	1.893	1.845	1.883	1.756	
	Ex	1.866	1.827	1.857	1.749	
R_{SiSi}	St	2.383	2.358	3.534	2.404	2.403
	Ex	2.374	2.349	3.489	2.400	2.398
R_{ISi}	St			2.531	2.512	2.510
	Ex			2.505	2.488	2.486
∠ICN	St	180.0	120.6			
	Ex	179.4	120.6			
∠SiSi	St	10.6	0.43		0.32	0.32
	Ex	10.4	0.44		0.54	0.58
E_{rel}	St	−54.2	−192.9	−264.3	−344.5	−376.7
	Ex	−58.9	−191.0	−264.8	−351.9	−375.6

[a] "St" refers to the standard 6-31G(d) basis while "Ex" refers to the larger 6-311++G(2d,p) basis for the Si dimer atoms and the N and C species. The bound distances are in angstroms while the XCN and SiSi buckling angles are in degrees. The SiC distance for ICN3 is measured with respect to the Si dimer atom bound to the halide.

TABLE 2: Calculated B3LYP/6-31G(d) Adsorption Energies (kJ/mol) for XCN1, XCN2, XCN3, SiNC, and SiCN Adsorption Structures on Single-Dimer (1D) and Triple-Dimer (3D) Clusters[a]

		XCN1	XCN2	XCN3	SiNC	SiCN
I	1D	−54.2	−192.9	−264.3	−344.5	−376.7
	3D	−81.3	−180.6	−240.7	−337.1	−367.9
	% diff	−50.0	6.4	8.9	2.1	2.3
Br	1D	−51.0	−198.9	−303.3	−380.5	−413.4
	3D	−78.9	−187.1	−281.8	−375.7	−407.3
	% diff	−54.7	5.9	7.1	1.3	1.5
Cl	1D	−44.7	−202.3	−289.4	−365.3	−397.9
	3D	−72.5	−189.9	−266.0	−359.0	−390.3
	% diff	−62.2	6.1	8.1	1.7	1.9

[a] Percent differences are with respect to the single-dimer energy. Negative percent differences indicate that the triple dimer is lower in energy.

with careful studies of ammonia adsorption on silicon clusters, the 6-31G(d) results are within 4 kJ/mol of the larger 6-311++G(2d,p) basis set.[26] Similar results are also found for methylamine adsorption on Si single-dimer clusters.[4,24] Thus, all further calculation are performed at the B3LYP/6-31G(d) level.

The computed adsorption energies for these five stable ICN, BrCN, and ClCN adsorption structures on both single- and triple-dimer clusters are listed in Table 2. For the triple-dimer cluster, the middle dimer is used for the adsorption site, while the two end dimers are bare. As an example, the triple-dimer XCN1 geometry is illustrated in Figure 3. Since the formation of the XCN end-on adsorption structure (XCN1) from gas-phase ICN, BrCN, and ClCN does not require bond cleavage, no adsorption barrier is expected. On the single cluster, the adsorption is exothermic with total energy changes of −54.2, −51.0, and −44.7 kJ/mol for ICN, BrCN, and ClCN, respectively (see Table 2). With increasing halide electronegativity, the energy change decreases by a small amount. One explanation is that with the increased electronegativity of the halide, there is a decrease in the electron density that the nitrogen atom can donate to the dative bond. The net result is a reduction in the adsorption energy. These results are consistent with the calculated −49.6 kJ/mol adsorption energy for an analogous HCN structure.[16] A

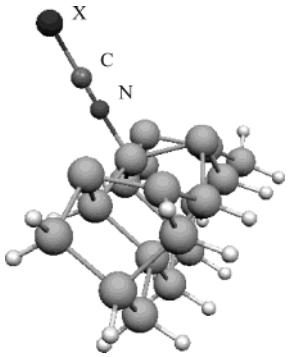

Figure 3. XCN1 adsorption model utilizing the Si triple-dimer cluster.

lower adsorption energy of −69.6 kJ/mol is calculated using B3LYP/6-31G(d) for acetonitrile (CH_3CN)[33] and is possibly due to the electron-donating ability of the CH_3 group as compared to H or halide substitution. The single-dimer XCN adsorption energies are also less than the −96.2 kJ/mol value for ammonia, calculated using B3LYP/6-311++G(2df,2pd) and a single-dimer cluster,[26] or the −120 to −90 kJ/mol range found for methyl-, dimethyl-, and trimethylamines calculated using a single-dimer cluster and B3LYP with varying basis sets.[4,24,25] The sp^3 N in both ammonia and amines appears to be able to form a stronger bond by donating more charge to the Si dimer atom than the sp N in the CN triple-bonded species. This effect is consistent with the decreasing electron donor strengths due to the increasing s character of the lone pair.[34]

Utilizing a triple-dimer cluster for ICN1, BrCN1, and ClCN1, the adsorption energy for XCN1 is consistently found to be 27−28 kJ/mol lower (see Table 2) than that of a single dimer. These differences correspond to a 50% error with respect to the single-dimer results. Thus, the total electronic energy of the dative bond structure is strongly dependent on the cluster size. For molecular ammonia adsorption, a 25 kJ/mol difference is found between a single dimer and larger clusters using B3LYP/6-31G(d),[26] while a 28 kJ/mol difference is found using B3LYP/6-311+G(2d,p).[24] This energy difference is attributed to a greater ability of the larger clusters to delocalize the additional density created by the dative bond along the dimer row.[26] For the analogous HCN configuration, Bacalzo-Gladden et al. find an energy difference, including zero-point corrections, of 28 kJ/mol between the single- and double-dimer silicon clusters.[7] From these results, the magnitude of the cluster size effect appears to depend only on the presence of a dative bond and is relatively independent of the substitution on the nitrogen atom.

For XCN1, the geometric parameters (see Table 3) obtained from both single- and triple-dimer clusters are practically identical. In the XCN1 geometries, the CN bond length is only 0.04 Å greater than the gas-phase value, indicating that the CN triple bond is intact. In all cases, the nitrogen lone pair forms a dative bond between the nitrogen end of the XCN molecule and the electrophilic (buckled-down) Si generated by an 11−12° buckling of the Si dimer. The magnitude of the buckling is virtually independent of XCN species and cluster size. These buckling angles are consistent with 13° buckling found for ammonia[26−28] and the 10° buckling found for methylamines.[24]

The XCN2 species are generated by the reaction of XCN1 across the Si dimer to achieve an intermediate side-on configuration. This 1,2-dipolar addition of the CN group across the Si dimer bond results in a four-membered Si_2NC ring. Although geometries analogous to XCN2 formed by adsorption either across the dimer rows or between two dimer bonds in the same row may be possible, only geometries based on single-dimer

TABLE 3: Calculated B3LYP/6-31G(d) Geometries for XCN1 and XCN2 Adsorption Structures on Single-Dimer (1D) and Triple-Dimer (3D) Clusters[a]

		XCN1			XCN2		
		I	Br	Cl	I	Br	Cl
R_{XC}	1D	2.004	1.770	1.624	2.240	1.964	1.793
	3D	1.996	1.767	1.622	2.241	1.963	1.792
R_{CN}	1D	1.162	1.162	1.161	1.264	1.271	1.274
	3D	1.161	1.161	1.160	1.262	1.269	1.272
R_{SiC}	1D				1.953	1.943	1.951
	3D				1.955	1.945	1.952
R_{SiN}	1D	1.893	1.894	1.903	1.845	1.839	1.834
	3D	1.880	1.881	1.889	1.858	1.851	1.846
R_{SiSi}	1D	2.383	2.386	2.384	2.358	2.358	2.355
	3D	2.399	2.399	2.398	2.335	2.335	2.333
∠XCN	1D	180.0	180.0	180.0	120.6	121.0	120.7
	3D	180.0	180.0	180.0	121.1	121.5	121.0
∠SiSi	1D	10.6	10.7	10.8	0.43	0.39	0.47
	3D	11.5	11.6	11.7	0.12	0.17	0.12

[a] Bond distances are in angstroms, while the XCN and Si−Si buckling angles are in degrees.

cluster models are considered in this investigation. For phenyl isothiocyanate,[12] acetonitrile[13,14,33,35] and benzonitrile[15] on the Si(100) surface, 1,2-dipolar addition reactions that result in a four-membered Si_2NC ring are theoretically predicted and experimentally observed.

The calculated energy difference (see Table 2) between the single- and triple-dimer XCN2 models is 12 kJ/mol. In contrast to the XCN1 results, this represents only a 6% error with respect to the single-dimer result. Importantly, the adsorption energies of the triple-dimer cluster models are always smaller than that found for the single dimer. Unlike XCN1, the Si dimer atoms are unbuckled. For NH_3 adsorption, the additional strain energy due to the unbuckling is better described by the triple-dimer cluster and results in a 12 kJ/mol decrease in adsorption energy for the dissociated structures.[26] For XCN2, a similar 12 kJ/mol decrease (see Table 2) in the adsorption energy is observed with the triple-dimer clusters. The XCN2 geometric parameters (see Table 3) for the single- and triple-dimer clusters are practically identical. With the exception of the expected changes in the XC bond length, all of the XCN2 structures are geometrically similar. The CN bond is significantly longer (1.26−1.27 Å), indicating a CN double bond. Thus, even if direct adsorption into the XCN2 state is possible, a barrier due to the partial breaking of the CN triple bond is expected.

Table 4 lists the optimized geometric parameters obtained for the dissociated adsorption structures (XCN3, SiNC, SICN) on single- and triple-dimer clusters. Since creating these structures requires bond breaking, no barrierless adsorption channel from XCN in the gas phase into the XCN3, SiCN, or SiNC state is expected. The XCN3 model for XCN adsorption was not originally considered in the study of ICN adsorption.[16] Internal reaction coordinates studies (see below) revealed this unexpected stable intermediate species. The adsorption energy of this species (see Table 2) is between XCN2 and SiNC. Similar to XCN2, only a small 8% difference is found between the single-dimer clusters and triple-dimer clusters. The geometric parameters (see Table 4) are also insensitive to cluster size effects. In this structure, the C atom of the CN species inserts between the two Si dimer atoms. In studies of ammonia decomposition on Si single-dimer clusters, the N atom of an NH species can insert itself between the two Si dimer atoms.[28] Both the weakness of the Si dimer bond compared to other Si−Si bonds connecting the dimer atoms to the rest of the cluster and the reduction of strain energy from the mismatch between the Si−N and the Si−Si bond lengths result in the Si dimer insertion structure having the lowest energy compared to all other possible insertion geometries.[28] For XCN3, a similar argument can also be made for the insertion into the Si dimer bond and not into the Si−Si backbone. As in the case of the side-on XCN2 species, the CN bond length implies that the CN bond has a double-bond character. Thus, the greater stability of this structure with respect to XCN2 is due to the formation of a strong SiX bond and two SiC bonds. Although the XC bond in XCN is stronger than the typical XC bond[36] due to the overlap between the p orbital on the halide and the π-system on the CN group, the formation of the XSi bond compensates for the loss of this bond. Thus, the main energetic difference between XCN3 and XCN2 is the formation of an additional SiC and the loss of the weaker Si dimer bond.

The SiNC and SiCN structures are energetically more stable than all other geometries. As in the case of XCN3, the XSi bond compensates for the loss of the XC bond. Thus, the additional stability of SiNC and SiCN structures is due to the retention of the CN triple bond and the Si dimer bond along with the creation of a strong SiN or SiC bond, respectively. In addition, the SiN and SiC bonds are shorter than those found in the XCN3 structure. For acetonitrile[14,33,35] and benzonitrile,[15] theoretical investigations of an analogous dissociated adsorption geometry was not attempted. The influence of the Si cluster size on the total energy of the SiNC and SiCN species is minimal. Only a small 2% difference in the adsorption energy relative to the single-dimer clusters is found for these dissocia-

TABLE 4: Calculated B3LYP/6-31G(d) Geometries for SiNC and SiCN Adsorption Structures on Single-Dimer (1D) and Triple-Dimer (3D) Clusters[a]

		XCN3			SiNC			SiCN		
		I	Br	Cl	I	Br	Cl	I	Br	Cl
R_{CN}	1D	1.258	1.260	1.260	1.186	1.185	1.186	1.165	1.165	1.165
	3D	1.257	1.258	1.259	1.186	1.186	1.186	1.165	1.165	1.165
R_{SiC}	1D	1.866	1.867	1.866				1.852	1.853	1.853
	3D	1.851	1.852	1.849				1.852	1.854	1.853
R_{SiN}	1D	1.883	1.883	1.883	1.756	1.758	1.757			
	3D	1.892	1.891	1.891	1.756	1.758	1.757			
R_{SiSi}	1D	3.534	3.536	3.531	2.404	2.400	2.404	2.403	2.400	2.400
	3D	3.460	3.471	3.453	2.387	2.383	2.387	2.386	2.382	2.386
R_{XSi}	1D	2.531	2.251	2.108	2.512	2.242	2.103	2.510	2.240	2.102
	3D	2.535	2.246	2.109	2.513	2.239	2.103	2.512	2.238	2.102
∠SiSi	1D				0.32	0.55	0.25	0.32	0.55	0.20
	3D				0.98	1.3	0.94	1.0	1.3	0.97

[a] The bond distances are in angstroms, while the SiSi buckling angles are in degrees. For XCN3, the SiC distance is measured with respect to the Si dimer atom bound to the halide.

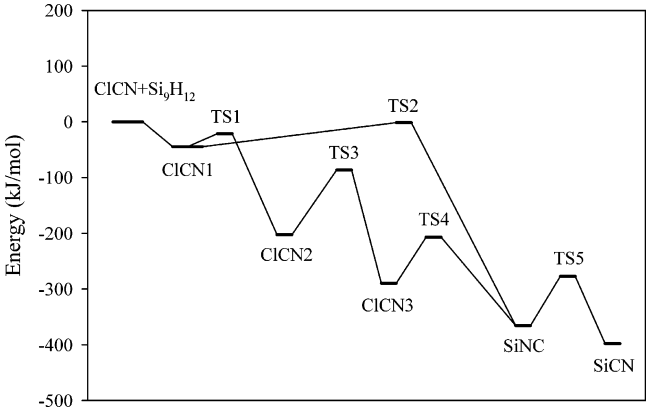

Figure 4. Potential energy profile for different adsorption modes of XCN and their transition states on Si single-dimer cluster. The solid line represents the primary pathways for the decomposition of XCN into adsorbed atomic X and molecular CN.

tion structures. As in the case of XCN2, the decrease in the adsorption energy for the triple-dimer clusters relative to that found for single-dimer clusters is attributed to the additional strain energy created by the unbuckled Si dimer.

The standard bond enthalpies of SiC and SiN are similar.[37] This similarity results in the relative closeness of the SiN and SiC adsorption energies. Computationally, the SiCN structure is on average 30 kJ/mol more stable than SiNC. A similar small energy difference is also found between the analogous HCN structures.[7] The bonding of the CN functional group in the SiNC and SiCN structures is independent of the halide that is bound to the opposite Si dimer atom. In both the SiNC and SiCN structures, the Si dimer is practically unbuckled. The CN bond lengths for SiNC and SiCN are 1.18 and 1.16 Å, respectively, indicating a triple-bond character. In addition, the optimized geometric parameters (Table 4) are similar for both the single- and triple-dimer calculations. At most, a 0.02 Å difference is found for the Si dimer bond length.

The adsorption of the INC isomer is discussed in ref 16. Based on HNC adsorption on a single-dimer cluster,[7] some consideration of the XNC configurations is required. For ICN, Kadossov et al. find that the analogous structure to XCN1 (XNC1) is unphysical due to an abnormally long IN bond length.[16] Similar results are found for both BrNC and ClNC. In addition, an intermediate side-on configuration structure analogous to XCN2 (XNC2) is also found for ICN.[16] For ICN, there is a large barrier between the lowest energy SiCN species and the XNC2 species. In addition, the energy of the XNC2 species is only slightly below the transition state energy between SiCN and XNC2. Thus, these analogous XNC adsorption geometries are not expected to play a role in the surface reaction chemistry of XCN and are therefore not considered further.

Adsorption and Dissociation Pathways. The reaction pathways between the various ClCN single-dimer derived adsorption configurations, along with the computed transition state energies, are shown in Figure 4. Due to the similarity, the reaction pathways for ICN and BrCN on Si single-dimer clusters are not shown. For XCN2, although reaction pathways in which the halide is transferred to an adjacent dimer row are geometrically possible, only reaction pathways which are possible on a single-dimer cluster are studied in this work. All transition states contain one imaginary frequency and are further verified using the internal reaction coordinate (IRC) option in Gaussian 98. This procedure[38,39] computes the lowest energy pathway from the given transition state to either the product or the reactant. Based on the eigenvector for the imaginary frequency,

TABLE 5: Calculated B3LYP/6-31G(d) Adsorption Energies (kJ/mol) for the Single-Dimer Transition State Models

	TS1	TS2	TS3	TS4	TS5
I	−38.4	−29.7	−116.2	−177.1	−255.6
Br	−25.2	−12.3	−106.1	−218.9	−292.4
Cl	−21.3	−1.5	−86.5	−206.9	−277.2

TABLE 6: Calculated B3LYP/6-31G(d) Geometries for TS1 and TS2 Transition States on a Single-Dimer (1D) Cluster[a]

	TS1			TS2		
	I	Br	Cl	I	Br	Cl
R_{XC}	2.230	1.812	1.653	2.538	1.850	1.689
R_{CN}	1.189	1.182	1.182	1.186	1.187	1.194
R_{SiN}	1.787	1.848	1.848	1.793	1.920	1.927
R_{SiSi}	2.418	2.405	2.408	2.333	2.326	2.315
∠XCN	139.4	156.1	153.3	131.0	141.7	141.2
∠SiSi	5.5	8.9	9.1	0.92	4.9	3.7

[a] The bond distances are in angstroms, while the XCN and SiSi buckling angles are in degrees.

we had previously assumed that there is only one transition state between XCN2 and SiCN.[16] However, IRC calculations for the less demanding ClCN system revealed the presence of an additional stable intermediate species, XCN3. As discussed above, the formation of the XCN3 species involves cleavage of the Si dimer bond. Thus, the pathway starting from side-on bonded species (XCN2) to the dissociated SiNC species is more complex than originally assumed.[16]

The primary pathway from the gas phase XCN species to the lowest energy of the dissociated structure, SiCN, is shown as a solid line in Figure 4. Table 5 reports the single-dimer transition state energies, while Tables 6 and 7 list the geometric parameters. Since the total energy of XCN1 depends strongly on the size of the cluster, the first two transition states (TS1 and TS2) are also optimized using the triple-dimer cluster model. For TS1, a 12 kJ/mol difference is found between the single- and triple-dimer clusters, approximately a 50% average error between the two clusters. Such a large error could be anticipated given the cluster size effects found for XCN1 and the resemblance of the TS1 structure to that of XCN1. Similar to XCN1, the transition state energy for TS1 is consistently lower for the larger clusters. In contrast, a relatively small difference of 1 kJ/mol is found for TS2. The other transition states, TS3, TS4, and TS5, are between the stable XCN2, XCN3, SiNC, and SiCN species, respectively. These stable species are essentially unaffected by the size of the silicon cluster. Therefore, only single-dimer calculations are performed on the transition states.

At room temperature, UPS and XPS measurements indicate that molecular ICN, BrCN, and ClCN dissociate upon exposure to the Si(100) surface and form an atomic halide and molecular CN species.[10,11] Assuming that the reaction pathways shown in Figure 4 are followed experimentally, some tentative conclusions can be inferred. The initial dative bonded end-on adsorption structure (XCN1) is expected to form via a barrierless transition state. Similar conclusions have been drawn for other dative bonded species such as HCN, acetonitrile, ammonia, and various amines.[4,7,17,24−26,28,33] Assuming that kinetic energy gained through adsorption can be utilized, ICN1 and BrCN1 can react, through transition state TS2, to form SiNC directly. The small buckling of the Si dimer atoms in TS2 (see Table 6) indicates a relatively weak dative bond. In addition, the XCN molecule is bent and the CN bond is slightly (0.02 Å) elongated with respect to that found for gas-phase XCN. Due to the strength of the ClC bond, the transition state (TS2) between ClCN1 and SiNC is only 1.5 kJ/mol less than the energy of the isolated

TABLE 7: Calculated B3LYP/6-31G(d) Geometries for TS3, TS4, and TS5 Transition States on Single-Dimer Clusters[a]

	TS3			TS4			TS5		
	I	Br	Cl	I	Br	Cl	I	Br	Cl
R_{CX}	2.873	2.520	2.434						
R_{CN}	1.220	1.221	1.219	1.222	1.224	1.223	1.191	1.190	1.191
R_{SiC}	1.865	1.849	1.848	2.124	2.108	2.126	2.022	2.020	2.022
R_{SiN}	1.939	1.944	1.947	1.875	1.873	1.874	2.110	2.120	2.116
R_{SiSi}	2.468	2.471	2.471	2.529	2.547	2.549	2.404	2.399	2.404
R_{XSi}	3.205	2.905	2.820	2.628	2.305	2.154	2.510	2.240	2.101
∠XCN	140.7	141.0	140.5						

[a] The bond distances are in angstroms, and the XCN angles are in degrees.

ClCN molecule and the single-dimer cluster. For the triple-dimer cluster, the energy is greater than that for the isolated species by 2.9 kJ/mol. Thus, the pathway between ClCN1 and SiNC through TS2 is unlikely. For ICN and BrCN, the adsorption energy of TS2 is negative and barrierless adsorption into this state may be possible. Thus, SiNC could be formed directly from the gas phase via TS2. If SiNC via TS2 is energetically possible, the resulting kinetic energy gained is more than sufficient to overcome the barrier between SiNC and the final experimentally observed product, SiCN. An examination of the transition state structure TS5 (referred to as TS4 in ref 16) between SiNC and SiCN reveals a partial breaking of the SiN bond before the SiC bond fully forms, which results in the 90 kJ/mol barrier. Supporting this conclusion, the barrier height is also independent of the halide.

The second pathway to form SiCN involves a 1,2-dipolar addition reaction of XCN1 across the Si dimer to achieve an intermediate side-on configuration, XCN2, through TS1. The Si dimer atoms in the TS1 geometry (see Table 6) are buckled by approximately 8°. In addition, XCN molecule is dative bonded to the electrophilic (buckled-down) Si dimer atom. Thus barrierless adsorption into TS1, followed by the direct formation of XCN2, may be possible. Similar conclusions have been reached for HCN[7,17] and CH_3CN.[33] Assuming that the single-dimer pathway represents the experimental pathway and given that the experimental species formed at room temperature is SiCN,[10,11] the newly created XCN2 species must possess sufficient energy to overcome TS3, TS4, and TS5. If there is no thermal accommodation of the XCN2, this species will have enough kinetic energy to form XCN3 through TS3. The newly formed XCN3 species can use the kinetic energy gained from the previous reaction (again, assuming no thermal accommodation) to further reaction through TS4 giving SiNC. Finally, SiNC contains more than sufficient kinetic energy to overcome the barrier between SiNC and SiCN, the experimentally observed product. Given the calculated barrier height, it is reasonable to assume that the reaction proceeds to the experimentally observed SiCN species at room temperature.[10,11] The driving force for the formation of this dissociated species is the replacement of the XC bond with the stronger XSi and SiC bonds.

The 1,2-dipolar addition reaction products from acetonitrile[13,14] and benzonitrile[15] on the Si(100) surface are experimentally observed. For acetonitrile, an adsorbed CH_3 group replaces the halide in the analogous SiCN geometry. Unlike the XCN, SiCN species where a strong XSi bond replaces a weaker XC bond, the formation of an analogous dissociated species from the nitriles requires that a strong CC bond is replaced by weaker SiC bond. In addition, a large activation energy is expected due to the need to break a CC bond. Thus, in contrast with XCN, the 1,2-dipolar addition reaction products from acetonitrile and benzonitrile are stable. For HCN, a stable side-on structure surrounded by transition state barriers larger than the adsorption energy is predicted.[7,17] The stronger HC bond with respect to the HSi bond gives the analogous HCN structure greater stability than that of XCN2. For XCN2, a low barrier reaction pathway driven by the formation of a strong XSi bond destabilizes this structure. In addition, a side-on adsorbed HCNH species is observed experimentally for HCN adsorption on Si(100) surfaces.[40] In contrast, an analogous species is not observed in UPS and XPS studies of XCN adsorption on Si(100) surfaces.[10,11] For HCN, surface H liberated by the formation of CN functional groups can further react with other adsorbed HCN molecules, leading to the HCNH species on the Si(100) surface. The formation of HCNH from the interaction between two HCN molecules on double-dimer clusters has been studied theoretically.[17] The formation of an HCNH species and a CN function group on a double dimer is only 4 kJ/mol greater than two isolated side-on adsorbed species. The formation of the additional HN bond in HCNH counterbalances the loss of the HC bond required to form the separately adsorbed CN functional group. Unlike HCNH, XCNX side-on species is expected to be energetically unstable with respect to separately adsorbed halides and CN functional group due to the stronger XSi bond as compared to either the XC or XN bond.

Conclusions

The adsorption and surface reactions of ICN, BrCN, and ClCN on the Si(100)−(2×1) surface are studied using ab initio quantum calculations on single- and triple-dimer clusters. These cyanogen halides can physisorb into an end-on molecular species that is bound through the N to the Si cluster via dative bond. The adsorption energy of this dative bonded species is sensitive to the cluster size, with the lowest energy obtained using a triple-dimer cluster. This species can further react to form either an adsorbed CN group with the N bond to the surface or a side-on intermediate by reacting across the Si dimer bond. For ClCN, the energy of the transition state for the former process is close to that of the isolated molecule and cluster. The N-bonded CN species can subsequently rotate to form a C-bonded CN group. Of the two possible orientations, the C-bonded species is found to have the lowest adsorption energy. Once the first barrier to form the N-bonded CN species is overcome, no significant transition state barriers are present.

The side-on intermediate can react to form an additional structure in which the halide−carbon bond is broken and the C end of the CN group inserts into the Si dimer bond. This reaction is facilitated by the formation of both a strong XSi bond and a strong SiC bond. The insertion species can further react to form triple-bonded CN species adsorbed through the N atom by recreating the Si dimer bond. Finally, this newly created species can reorient itself to form a C-bonded CN species. After the side-on species is formed from the dative bonded species, no significant barriers are present. Thus, for both pathways, the lowest energy structure is expected to form in agreement with experimental studies.[10,11]

Acknowledgment. The authors acknowledge the support of this work by Oklahoma State University Center for Energy Research and by the Research Corporation.

References and Notes

(1) Bent, S. F. *Surf. Sci.* **2002**, *500*, 879.
(2) Yates, J., Jr. *Science* **1998**, *279*, 335.
(3) Lu, X.; Lin, M. C. *Int. Rev. Phys. Chem.* **2002**, *21*, 137.
(4) Mui, C.; Wang, G. T.; Bent, S. F.; Musgrave, C. B. *J. Chem. Phys.* **2001**, *114*, 10170.
(5) Cao, X.; Coulter, S. K.; Ellison, M. D.; Liu, H.; Liu, J.; Hamers, R. J. *J. Phys. Chem. B* **2001**, *105*, 3759.
(6) Cao, X.; Hamers, R. J. *J. Am. Chem. Soc.* **2001**, *123*, 10988.
(7) Bacalzo-Gladden, F.; Musaev, D. G.; Lin, M. C. *J. Chin. Chem. Soc. (Taipei)* **1999**, *46*, 395.
(8) Bu, Y.; Ma, L.; Lin, M. C. *J. Phys. Chem.* **1995**, *99*, 1046.
(9) Bu, Y.; Ma, L.; Lin, M. C. *J. Phys. Chem.* **1993**, *97*, 7081.
(10) Rajasekar, P.; Kadossov, E. B.; Watt, T.; Materer, N. F. *Surf. Sci.* **2002**, *515*, 421.
(11) Rajasekar, P.; Kadossov, E. B.; Ward, L.; Baker, J. L.; Materer, N. F. *J. Phys. Chem. B* **2003**, *107*, 7726.
(12) Ellison, M. D.; Hamers, R. J. *J. Phys. Chem. B* **1999**, *103*, 6243.
(13) Bournel, F.; Gallet, J. J.; Kubsky, S.; Dufour, G.; Rochet, F.; Simeoni, M.; Sirotti, F. *Surf. Sci.* **2002**, *513*, 37.
(14) Tao, F.; Wang, Z. H.; Qiao, M. H.; Liu, Q.; Sim, W. S.; Xu, G. Q. *J. Chem. Phys.* **2001**, *115*, 8563.
(15) Tao, F.; Wang, Z. H.; Xu, G. Q. *J. Phys. Chem.* **2002**, *106*, 3557.
(16) Kadossov, E. B.; Rajasekar, P.; Materer, N. F. *Chem. Phys. Lett.* **2003**, *370*, 548.
(17) Bacalzo-Gladden, F.; Lu, X.; Lin, M. C. *J. Phys. Chem. B* **2001**, *105*, 4368.
(18) Frisch, M. J.; Trucks, G. W.; Schlegel, H. B.; Scuseria, G. E.; Robb, M. A.; Cheeseman, J. R.; Zakrzewski, V. G.; Montgomery, J. A.; Stratmann, R. E.; Burant, J. C.; Dapprich, S.; Millam, J. M.; Daniels, A. D.; Kudin, K. N.; Strain, M. C.; Farkas, O.; Tomasi, J.; Barone, V.; Cossi, M.; Cammi, R.; Mennucci, B.; Pomelli, C.; Adamo, C.; Clifford, S.; Ochterski, J.; Petersson, G. A.; Ayala, P. Y.; Cui, Q.; Morokuma, K.; Malick, D. K.; Rabuck, A. D.; Raghavachari, K.; Foresman, J. B.; Cioslowski, J.; Ortiz, J. V.; Baboul, A. G.; Stefanov, B. B.; Liu, G.; Liashenko, A.; Piskorz, P.; Komaromi, I.; Gomperts, R.; Martin, R. L.; Fox, D. J.; Keith, T.; Al-Laham, M. A.; Peng, C. Y.; Nanayakkara, A.; Gonzalez, C.; Challacombe, M.; Gill, P. M. W.; Johnson, B.; Chen, W.; Wong, M. W.; Andres, J. L.; Gonzalez, C.; Head-Gordon, M.; Replogle, E. S.; Pople, J. A. *Gaussian 98*, Revision A.7; Gaussian Inc.: Pittsburgh, PA, 1998.
(19) Becke, A. D. *J. Chem. Phys.* **1993**, *98*, 5648.
(20) Lee, C.; W. Y.; Parr, R. G. *Phys. Rev. B* **1988**, *37*, 785.
(21) Francl, M. M.; Pietro, W. J.; Hehre, W. J.; Binkley, J. S.; Gordon, M. S.; DeFrees, D. J.; Pople, J. A. *J. Chem. Phys.* **1982**, *77*, 3654.
(22) Dunning, T. H.; Hay, P. J. In *Modern Theoretical Chemistry*; Schaefer, H. F., Ed.; 1977; p 1.
(23) Hay, P. J.; Wadt, W. R. *J. Chem. Phys.* **1985**, *82*, 270.
(24) Carman, A. J.; Zhang, L.; Liswood, J. L.; Casey, S. M. *J. Phys. Chem.* **2003**, *107*, 5491.
(25) Kato, T.; Kang, S.-Y.; Xu, X.; Yamabe, T. *J. Phys. Chem. B* **2001**, *105*, 10340.
(26) Widjaja, Y.; Musgrave, C. B. *Surf. Sci.* **2000**, *469*, 9.
(27) Widjaja, Y.; Musgrave, C. B. *Phys. Rev. B* **2001**, *64*, 205303/1.
(28) Widjaja, Y.; Mysinger, M. M.; Musgrave, C. B. *J. Phys. Chem. B* **2000**, *104*, 2527.
(29) Petrie, S. *Phys. Chem. Chem. Phys.* **1999**, *1*, 2897.
(30) Townes, C. H.; Holden, A. N.; Merritt, F. R. *Phys. Rev.* **1948**, *74*, 1113.
(31) Lee, T. J.; Martin, J. M. L.; Dateo, C. E.; Taylor, P. R. *J. Phys. Chem.* **1995**, *99*, 15858.
(32) Lafferty, W. J.; Lide, D. R.; Toth, R. A. *J. Chem. Phys.* **1965**, *43*, 2063.
(33) Lu, X.; Xu, X.; Wu, J.; Wang, N.; Zhang, Q. *New J. Chem.* **2002**, *26*, 160.
(34) Bent, H. A. *Chem. Rev.* **1960**, *61*, 275.
(35) Cho, J.-H.; Kleinman, L. *J. Chem. Phys.* **2003**, *119*, 6744.
(36) Davis, D. D.; Okabe, H. *J. Chem. Phys.* **1968**, *49*, 5526.
(37) Dean, J. A. *Lange's Handbook of Chemistry*, 14th ed.; McGraw-Hill: New York, 1992.
(38) Gonzalez, C.; Schiegel, B. *J. Phys. Chem.* **1990**, *94*, 5523.
(39) Gonzalez, C.; Schiegel, B. *J. Chem. Phys.* **1989**, *90*, 2154.
(40) Bu, Y.; Ma, L.; Lin, M. C. *J. Phys. Chem.* **1993**, *97*, 11797.